Received: 29 September 2017 | Revised: 12 January 2018 | Accepted: 27 February 2018 | Published on: 1 April 2018

DOI: 10.1002/joc.5514

International Journal of Climatology RMetS

RESEARCH ARTICLE

Tree-ring-based precipitation reconstruction in the source region of Weihe River, northwest China since AD 1810

Changfeng Sun[1,2] | Yu Liu[1,2,3,4] | Huiming Song[1,4] | Ruochen Mei[1,5] | Paramate Payomrat[1,5] | Lu Wang[1,5] | Ruoshi Liu[2]

[1]The State Key Laboratory of Loess and Quaternary Geology, Institute of Earth Environment, Chinese Academy of Sciences, China

[2]Department of Earth and Environmental Science, School of Human Settlements and Civil Engineering, Xi'an Jiaotong University, China

[3]Qingdao National Laboratory for Marine Science and Technology, Qingdao, China

[4]Interdisciplinary Research Center of Earth Science Frontier (IRCESF) and Joint Center for Global Change Studies (JCGCS), Beijing Normal University, Beijing, China

[5]University of Chinese Academy of Sciences, Beijing, China

Correspondence
Yu Liu, The State Key Laboratory of Loess and Quaternary Geology, Institute of Earth Environment, Chinese Academy of Sciences, Xi'an 710061, China.
Email: liuyu@loess.llqg.ac.cn

Funding information
National Natural Science Foundation of China, Grant/Award Number: 41401060, 41630531; CAS Key Research Program of Frontier Sciences, Grant/Award Number: GJHZ1777, XDPB05, QYZDJ–SSW–DQC021; Youth Innovation Promotion Association CAS; Project of State Key Laboratory of Loess and Quaternary Geology; Key Project of IEECAS

A tree-ring width chronology of *Picea purpurea* Mast from Mt. Shouyang in the source region of Weihe River (SWR), northwest China, was developed in this study. Correlation analysis showed that the precipitation from previous August to current July was the limiting climate factor of tree growth. Using a reliable and stable linear regression model, which explained 42.6% of the variance of the actual precipitation during the calibration period from 1958 to 2014, a 205-year long precipitation series was reconstructed for the SWR. The dry years in the reconstruction were well supported by historical documents, and famous historical droughts were also recorded in the dry periods of a low-frequency scale of the reconstructed precipitation. As demonstrated by the spatial correlation patterns, the reconstructed series compared well with other hydroclimate records for northwest China, indicating that it could represent large-scale hydroclimate changes. The 2–8-year interannual cycles and the interdecadal quasiperiods of 15.9 years and 18.6 years revealed that the precipitation in this region was probably affected by the El Niño-Southern Oscillation and North Atlantic Oscillation. The dry/wet years corresponded well with the El Niño/La Niña events and the SWR commonly experienced droughts during the low periods of North Atlantic Oscillation.

KEYWORDS

Mt. Shouyang, *Picea purpurea* Mast, precipitation reconstruction, source region of Weihe River, tree-ring width

1 | INTRODUCTION

Despite previous achievements in tree-ring-based climate reconstruction in northwest China (Liu *et al.,* 2005; 2013a; 2013b; Li *et al.,* 2006a; Yang *et al.,* 2011; Fang *et al.,* 2012; Sun and Liu, 2012; Song *et al.,* 2013; Zhang *et al.,* 2013; Chen *et al.,* 2015; Gou *et al.,* 2015), relevant studies in the source region of Weihe River (SWR), an important tributary of the Yellow River, are virtually non-existent. Conducting a tree-ring reconstruction in the SWR would undoubtedly help elucidate local climate change and, more importantly, improve the current understanding of the climate and environment of the Weihe and the Yellow Rivers.

Weiyuan is in the transition zone between the Loess Plateau and Tibetan Plateau, and it has a continental climate influenced by both the westerlies and the Asian monsoon (Yao *et al.,* 2011; Wang *et al.,* 2015). It is well known that the El Niño-Southern Oscillation (ENSO) has a significant relationship to the Asian monsoon (Wang, 2006), and the North Atlantic Oscillation (NAO) is closely connected with the westerlies (Scaife *et al.,* 2005). However, the relationships between the SWR climate and the ENSO and NAO over the past several centuries are still unclear. In addition,

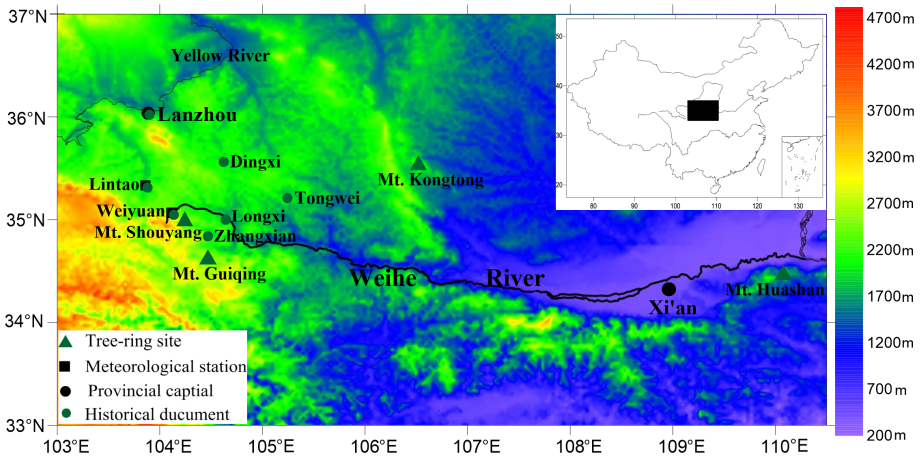

FIGURE 1 Location of tree-ring sites and meteorological stations. This map was created using the surfer version 10.3 software. The bold black line represents the Weihe River [Colour figure can be viewed at wileyonlinelibrary.com]

more high-resolution climate reconstructions based on individual sampling sites are required to better understand the full perspective of climate variability in northwest China. Li *et al*. (2015) noted that climate reconstructions from individual sampling sites were still of great importance because it was difficult to conduct regional reconstruction without sufficient individual reconstructions.

Therefore, in this study, the tree-ring widths of *Picea purpurea* Mast from Mt. Shouyang in the SWR were first used to establish a tree-ring chronology in the SWR. Then, the limiting factor of tree growth was determined by climate response analysis, and changes in the precipitation over the past two centuries were reconstructed. Finally, the characteristics of the precipitation variations were analysed and the influences of ENSO and NAO were discussed.

2 | MATERIAL AND METHODS

2.1 | Sampling site and chronology development

The study region, the SWR, is in Weiyuan County, northwest China (Figure 1). According to the Weiyuan meteorological station, the mean annual temperature is 5.94 °C. January and July are the coldest (−7.23 °C) and hottest (17.30 °C) months of the year, respectively (Figure 2a). The annual precipitation is approximately 510 mm, which is mainly concentrated from May to September. The rainfall during the summer and autumn is characterized by short-period rainstorms, and there is less rainfall in the spring and winter. Because of considerable annual evaporation, spring and summer droughts often occur in the SWR (Wang, 2009). Mt. Shouyang with altitude from 2,186 to 2,590 m is located at the south of the SWR. Its lithology is mainly sandstone soil and it belongs to the West Qinling geosyncline zone, with undulating, steep hills and lush vegetation.

Our sampling site, Mt. Shouyang (SY, 34.99°N, 104.24°E, 2,350 m a.s.l.), is in the southern region of Weiyuan County, northwest China (Figure 1). The dominant tree species in the sampling site is *Picea purpurea* Mast. In August 2015, 40 tree-ring cores were collected from 20 healthy *Picea purpurea* with two cores from each tree. *Picea purpurea* is shade-tolerant tree species with sciophilous and hardy characteristics. This species is mainly distributed in eastern Qinghai, northern Sichuan and southern Gansu (Song and Wang, 2002). It is mixed with *Abies faxoniana* Rehd and *Picea crassifolia* Kom at Mt. Shouyang.

According to the standard dendrochronological method, after a series of treatments, all the cores were visually dated and then measured using the LINTAB measurement system with a precision up to 0.01 mm. The COFECHA program (Holmes, 1983) was used to control the quality of the cross-dating and exclude possibly false rings or missing rings. Cores

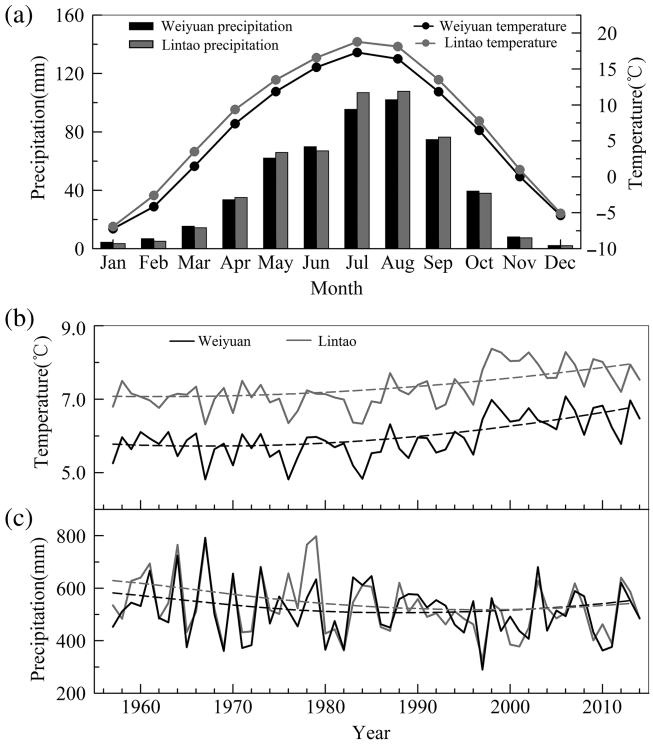

FIGURE 2 (a) Monthly precipitation and temperature of Weiyuan and Lintao meteorological stations (1957–2014). (b) Annual variations of temperature and (c) precipitation of Weiyuan and Lintao. The dotted lines in (b) and (c) represent the nonlinear trends of precipitation and temperature that were calculated using the ensemble empirical mode decomposition (EEMD) analysis (Wu *et al.*, 2009)

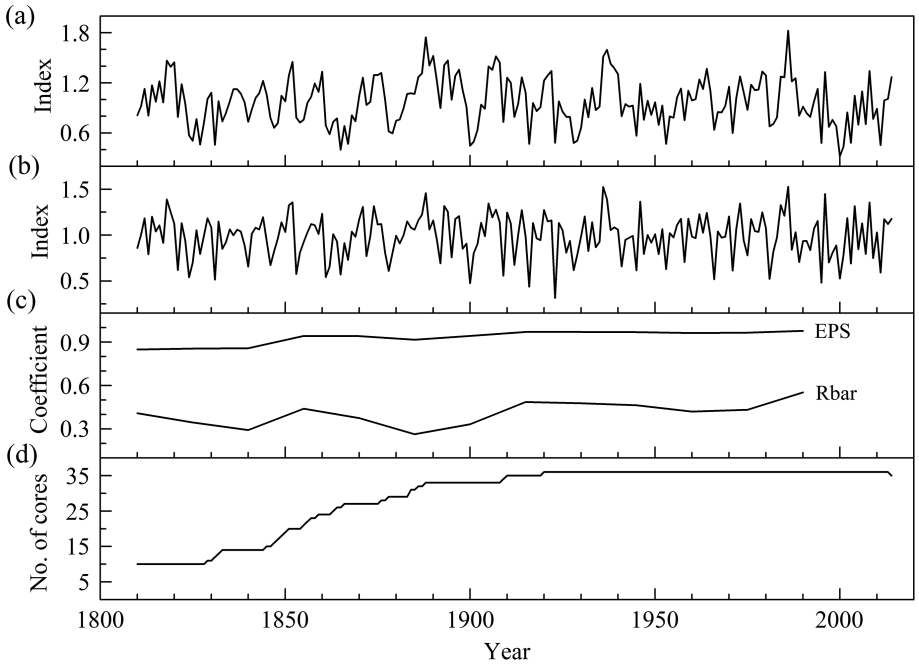

FIGURE 3 (a) Tree-ring standard (STD) chronology, (b) residual (RES) chronology, (c) running expressed population signal (EPS) and Rbar and (d) sample size

that were broken and cores with cross-dating ambiguities were excluded from further analysis. Finally, 36 cores from 20 trees were accurately cross-dated to their calendar year and used to establish the chronology. The COFECHA results showed that the average correlation coefficient among the individual series was 0.65 and the mean sensitivity was 0.34.

The ring-width chronology was produced by using the ARSTAN program (Cook, 1985). A negative exponential function or straight line was used to fit the trees' growth trend, and the stable variance technique was additionally used in developing chronology. The ARSTAN program produced three chronologies: standard (STD), residual (RES) and autoregressive (ARS). To further evaluate the quality of the ring-width chronology, Rbar and the expressed population signal (EPS) were calculated (Cook and Kairiukstis, 1990). Rbar is the correlation coefficient among the detrended ring-width indexes used for the chronology development. The EPS measures how well a limited-sample-size-based chronology approaches the theoretical chronology. An EPS value of 0.85 is generally considered to be the threshold for a reliable chronology (Wigley *et al.,* 1984), and the 1810–2013 AD period in our chronology reached this threshold, with a minimum of 10 cores (5 trees) contributing to the chronology in 1810 AD. Figure 3 shows the frequently used chronologies (STD and RES) in dendroclimatology.

2.2 | Meteorological data

The two nearest meteorological stations to the sampling site are Weiyuan (35.08°N, 104.12°E, 2111 m a.s.l., 1957–2014 AD) and Lintao (35.35°N, 103.85°E, 1894 m a.s.l., 1951–2014 AD). Figure 2 shows the temperature and precipitation of the two stations had similar variations. The correlations of the annual precipitation and temperature between the two stations are 0.82 and 0.94, respectively, during the period of 1957–2014 (Figure 2b and c). The ensemble empirical mode decomposition (EEMD) analysis (Wu *et al.,* 2009), an adaptive and temporally local time series analysis method designed for analysing non-linear and non-stationary climate data, showed that the trends of precipitation and temperature between the two stations were also similar. Compared to the Lintao station, the Weiyuan station is nearer to the sampling site and has a more similar elevation, so it was chosen to be used for the subsequent analysis.

2.3 | Statistics methods

A simple type of climatic response analysis, Pearson correlation analysis between the tree-ring chronology and meteorological data was used to explore how the climate influenced the radial growth of *Picea purpurea* and determine the climatic factor that limited tree growth. The past changes of the limiting climatic factor were then reconstructed by using a simple linear regression model based on ordinary least squares. The stability and reliability of the reconstruction function was checked by the split calibration-verification procedure (Meko and Graybill, 1995), using the Pearson's correlation coefficient (r), the coefficient of determination (R^2), the reduction of error (RE) and the coefficient of efficiency (CE; Cook *et al.,* 1999; Fritts, 1976). The RE and CE statistics test whether the model provides a more skilful estimate than the mean climatology of the calibration and verification periods, respectively, with positive values indicating the skill of the regression model (Cook *et al.,* 1999). In addition, multi-taper method spectral analysis (Thomson, 1982), a powerful tool in spectral estimation

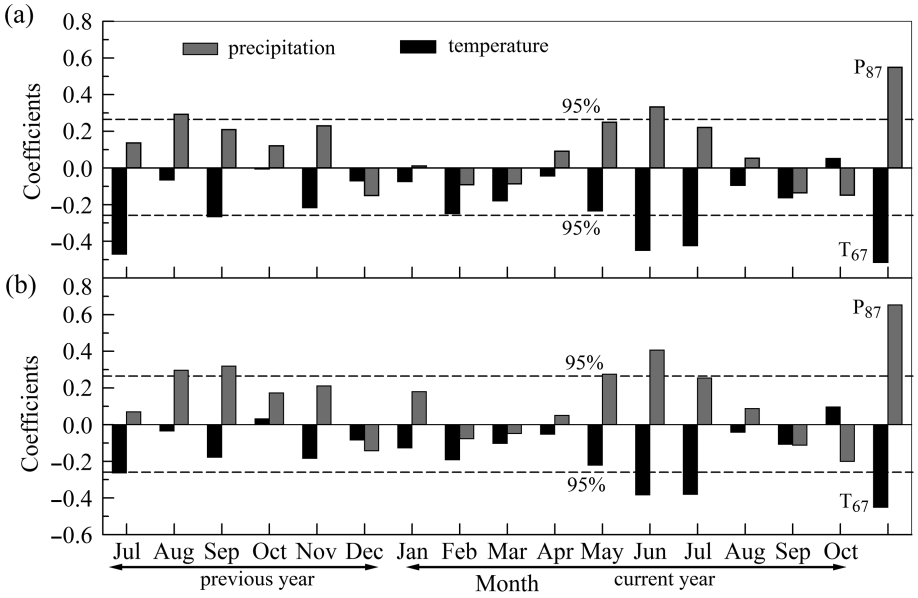

FIGURE 4 Correlation between the monthly climate and (a) the standard (STD) chronology as well as (b) the residual (RES) chronology during the period of 1958–2014. P_{87} is the precipitation from previous August to current July, and T_{67} is the temperature from June to July of current year. The dashed line is the 95% confidence limit

that is particularly effective for short time series, was conducted to identify the periodicity of the reconstructed climatic series. Spatial correlation analyses were adopted to represent the regional-scale climate signal variability by using the KNMI Climate Explorer (https://climexp.knmi.nl/start.cgi). The wavelet coherence analysis (Torrence and Compo, 1998) was used to analyse the relationship between the reconstructed precipitation and NAO.

3 | RESULTS

3.1 | Climate response

Tree ring-width growth of conifers in arid and semiarid sites was not only influenced by the climate during the growing season, and it was also affected by climatic conditions in autumn, winter, and spring prior to the growing season (Fritts, 1976). Therefore, the climate data from previous July to current October was collected to for the correlation analysis with chronologies. The response results (Figure 4) showed that both the STD and RES had positive correlations with precipitation and negative relationships with temperature, indicating that more rainfall and lower temperatures are, to some extent, beneficial to *Picea purpurea* growth. The STD chronology was significantly correlated with the precipitation of previous August and current June. Compared to precipitation, the relationship between the STD and temperature was more significant, with a correlation exceeding the 95% confidence level in previous July and September and current June and July. However, the RES chronology had a more significant relationship with precipitation than temperature (Figure 4). The correlations with the precipitation in previous August and September and current May and June passed the 95% significance level while the correlations with temperature in previous July and current June and July also exceeded 95% significance. Song and Wang (2002) noted that the cambium of *Picea purpurea* initiated activity at early May, and the early-wood formation was almost complete by the end of July. The season from May to July in the current year was the key period of trees growth. In this period, trees grow fast, and more rainfall is still beneficial to the cambial cell divisions. Precipitation was the highest in August, and temperature began to decrease (Figure 2). In this situation, the precipitation was enough for the tree growth of current year. Increased precipitation may improve photosynthesis and lead to more nutrient accumulation in the trees, which would benefit tree growth in the following year (Liu *et al.,* 2011).

In terms of tree growth, the seasonal climate played a more significant role over single month. After combining the monthly data, there were 126 groups for precipitation and temperature, respectively. It was found that both the STD and RES had the most significant relation with the precipitation from previous August to current July, with correlation coefficients of 0.549 and 0.653, respectively. The most significant correlation between temperature and both the STD and RES occurred during May–June, with coefficients of −0.515 and −0.452, respectively.

These results indicated that effect of precipitation on tree growth was greater than that of temperature. The limiting climatic factor for *Picea purpurea* was the precipitation from previous August to current July. It was also evident that the precipitation during this season was a limiting factor of tree growth in other regions of China (Li *et al.,* 2006b; Liu *et al.,* 2010; 2011; 2013a; Zhang *et al.,* 2011a; 2014; Tian *et al.,* 2012; Gao *et al.,* 2013). According to differences in the climate responses of the STD and RES, the RES chronology had a stronger precipitation signal. In addition, due to more high-frequency signal, RES chronologies have previously been used to reconstruct past precipitation change in China (Li *et al.,* 2006b; Chen *et al.,* 2013; 2015;

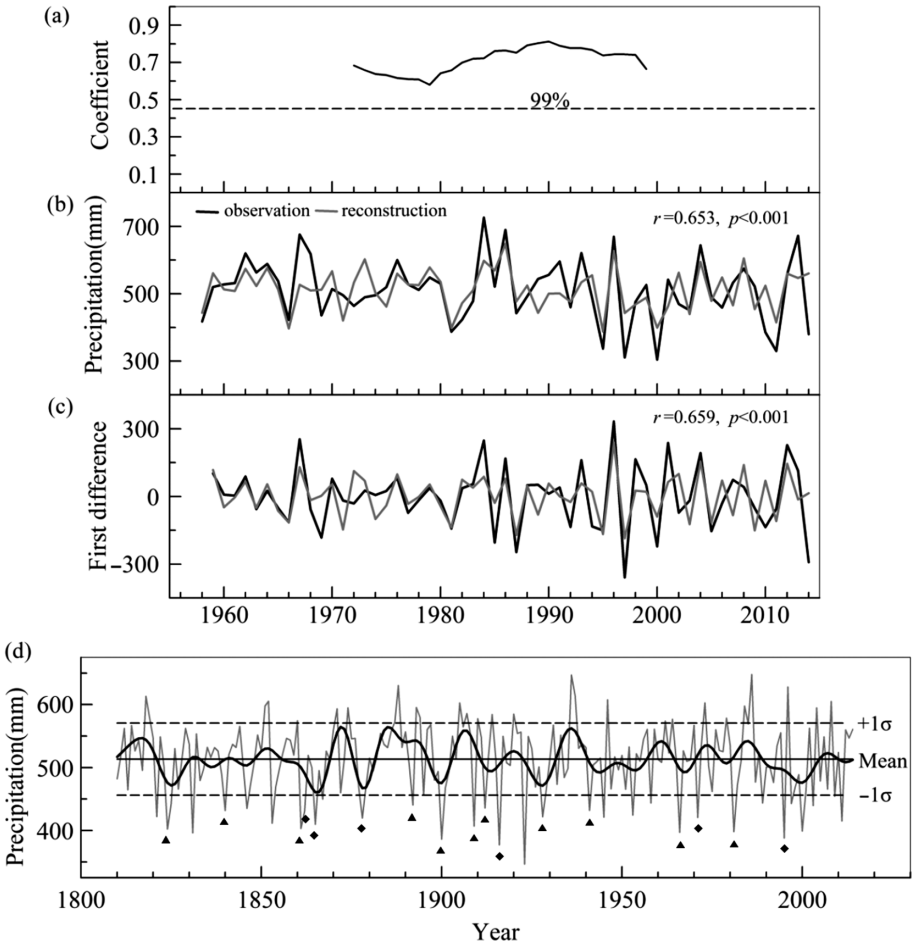

FIGURE 5 (a) Running correlation analysis between the residual (RES) chronology and observed P_{87}. (b) Comparisons between the reconstructed and observed precipitation during the period of 1958–2014 AD and (c) their first-order differences. (d) Reconstruction of precipitation during the period of 1810–2014. The bold line denotes a 10-year low-pass filter and the horizontal lines denote the mean and mean ± one standard deviation. The triangle and rhombus shapes indicate severe droughts and droughts, respectively, based on the dryness/wetness index in Lanzhou

Peng *et al.,* 2013; Zhang *et al.,* 2014). Therefore, the RES chronology of *Picea purpurea* from Mt. Shouyang was used to reconstruct the precipitation from previous August to current July (P_{87}). In addition, running correlation analysis between the RES chronology and P_{87} showed that the growth-climate signal had temporal stability (Figure 5a).

3.2 | Transfer function establishment and test

Based on the above analysis, the transfer function was designed using the simple linear regression model: $P_{87} = 248.515 * Wt + 268.118$.

($r = .653$, $R^2 = 42.6\%$, $R^2_{adj} = 41.6\%$, $n = 57$, $F = 40.901$, $p < 0.001$, D/W = 2.187,).

The Durbin-Watson statistic (D/W) was used to detect the presence of autocorrelation in the residuals from the regression analysis. Our D/W value was 2.19, indicating that there was no significant autocorrelation in the residuals (when $n = 57$, a D/W value between 1.62 and 2.38 indicates no autocorrelation).

The stability and reliability of the regression equation was verified using the split-sample method (Table 1). These validation trials were performed by dividing the common period (1958–2014) into two parts: 30 years for calibration (1958–1987/1985–2014) and 27 years for verification (1988–2014/1958–1984). The two rigorous verification statistics (RE and CE) were positive, indicating a rigorous model skill. All these statistical parameters showed that the regression model used in our reconstruction was very stable and reliable.

Our reconstruction could explain 42.6% of the observed variance during the calibration periods from 1958 to 2014. Figure 5b shows that the reconstruction closely tracked the observed precipitation. In addition, Figure 5c shows that the reconstructed and observed precipitation still had a significant relationship at high frequency by calculating the correlation coefficient between the first-order difference series of the reconstructed and observed precipitation.

3.3 | Precipitation reconstruction during the past 205 years for the SWR

Using the above transfer function, we reconstructed the precipitation from previous August to current July since 1810 AD (Figure 5d). For the past 205 years, the mean precipitation of the reconstruction was 513.3 mm and the standard deviation (σ) is 57.3 mm. We defined a dry year as the precipitation value lower than 456.0 mm (mean − 1σ), and a wet year as having a value higher than 570.6 mm (mean + 1σ). In the past 205 years, dry and wet years accounted for 16.1% (33 years) and 13.7% (28 years), respectively (Table 2). To analyse the low-frequency variation of the

TABLE 1 Calibration and verification statistics for the tree-ring reconstruction of the previous August to current July total precipitation

	Calibration (1958–1987)	Verification (1988–2014)	Calibration (1985–2014)	Verification (1958–1984)	Full calibration (1958–2014)
r	0.683[a]	0.616[a]	0.665[a]	0.629[a]	0.653[a]
R^2	0.466[a]	0.380[a]	0.442[a]	0.396[a]	0.426[a]
RE		0.415		0.400	
CE		0.360		0.345	

[a] Indicates the 99% confidence level.

reconstruction, a 10-year low-pass filter was applied (Figure 5d). After smoothing, there were several relative wet periods (1810–1820, 1870–1875, 1882–1896, 1903–1910, 1932–1940) and dry intervals (1821–1831, 1857–1869, 1876–1881, 1897–1902, 1923–1931, 1989–2003).

TABLE 2 Dry/wet years in the reconstructed precipitation and the El Niño/La Niña events (Gergis and Fowler, 2009)

Dry year	Precipitation (mm)	El Niño events	Wet year	Precipitation (mm)	La Niña events
1821	422.0		1818	613.3	
1824	402.3	M (1824)	1819	579.3	S (1819)
1825	442.1		1851	597.6	M (1851)
1831	396.1		1852	605.4	
1840	431.6		1860	574.5	VS (1860)
1846	435.1	VS (1845)	1871	593.4	VS (1871)
1853	411.5	VS (1853)	1874	594.9	S (1874)
1861	403.1		1887	572.3	VS (1887)
1862	430.9		1888	630.5	VS (1887)
1865	409.8	M (1865)	1893	595.4	VS (1893)
1867	449.8	VS (1866)	1894	579.8	E (1894)
1878	419.7	VS (1877)	1905	602.6	
1892	440.3	VS (1891)	1907	585.7	M (1907)
1900	386.2	VS (1900)	1910	577.8	VS (1910)
1909	406.8		1914	584.5	
1912	435.6	VS (1912)	1920	585.0	S (1918)
1916	377.2	VS (1915)	1936	647.1	
1923	346.6		1937	613.8	
1928	421.7	E (1926)	1946	607.6	S (1946)
1941	431.9	E (1941)	1962	573.8	M (1962)
1945	421.2	S (1944)	1964	576.8	M (1964)
1953	424.4	VS (1953)	1973	602.6	S (1973
1958	443.6	VS (1958)	1979	578.5	
1966	397.1	VS (1965)	1984	597.9	S (1984)
1971	420.5		1986	647.8	S (1985)
1981	398.1		1996	628.2	S (1996)
1989	443.6	E (1987)	2004	594.9	
1995	387.9	S (1994)	2008	605.1	VS (2008)
1997	442.8	E (1997)			
2000	399.1				
2003	439.6	S (2002)			
2009	454.3				
2011	415.0				

Magnitude classification of the El Niño/La Niña events: E = extreme; VS = very strong; S = strong; M = moderate.

Multi-taper method spectral analysis (Thomson, 1982) showed that the reconstructed precipitation contained 2.6–3.7-year and 7.9-year cycles at the 95% significance level and 2.4-year, 6.1-year, 15.9-year and 18.5-year quasi-periods (90% confidence level; Figure 6).

4 | DISCUSSIONS

4.1 | Characteristics of precipitation during the past 205 years

The dry years in the reconstructed series compared well with the drought events according to the dryness/wetness index in Lanzhou (Academy of Chinese Meteorological Science, 1981; Zhang *et al.*, 2003). There were 30 drought years during the period from 1810–2000 in our series and 17 years corresponded to drought events in Lanzhou (Figure 5d). In addition, many drought years in the reconstructed series could be found in historical documents (Compilation Committee of Dingxi County Annals, 1990; Compilation Committee of Longxi County Annals, 1990; Compilation Committee of Tongwei County Annals, 1990; Compilation Committee of Weiyuan County Annals, 1998; Compilation Committee of Lintao County Annals, 2001; Compilation Committee of Zhangxian County Annals, 2005). For example, in 1824, Dingxi, Lintao, Weiyuan, Tongwei, Longxi, Zhangxian and other counties were extremely dry and people suffered from famine. At Longxi, the famine was so terrible, only tree bark and grass roots could be eaten, countless people died of

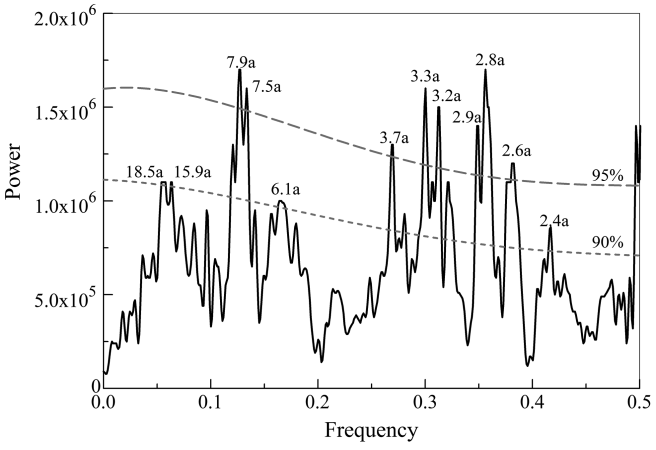

FIGURE 6 Spectrum analysis result of the reconstructed precipitation. The dashed line indicates the 95 and 90% confidence levels

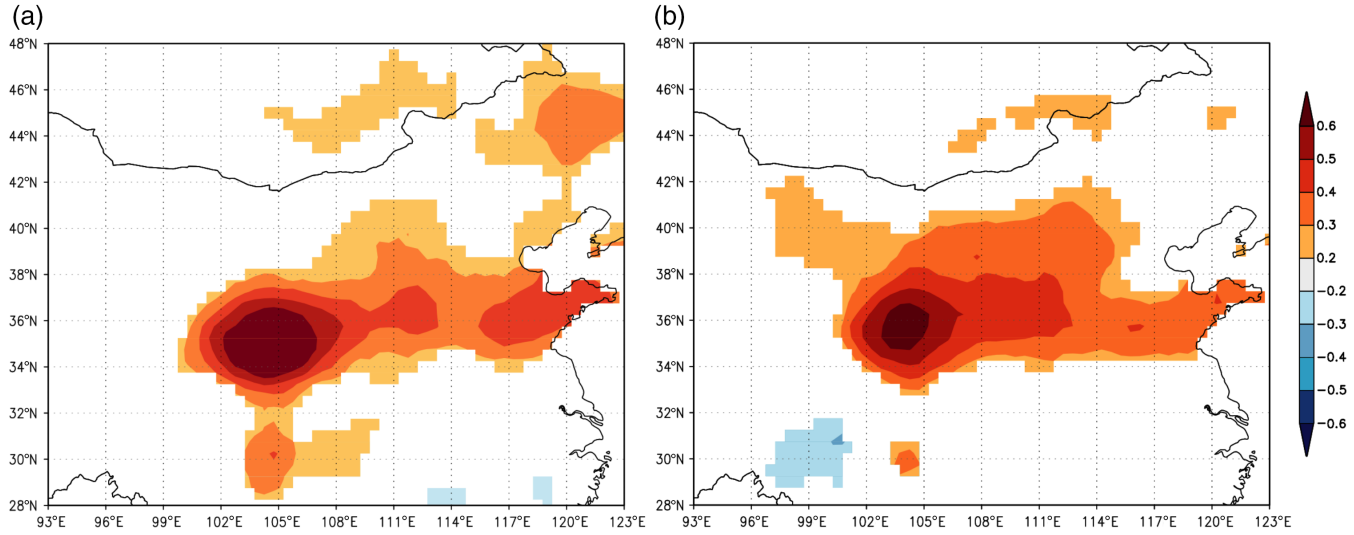

FIGURE 7 Spatial correlation between the CRU TS V4.00 grid precipitation data and (a) observed P_{87} and (b) our reconstructed P_{87} during the period of 1958–2014 [Colour figure can be viewed at wileyonlinelibrary.com]

hunger, and bodies were widespread. In 1867, Dingxi and Lintao experienced serious droughts, and cannibalism and famine were common. In 1878, Lintao, Dingxi, Weiyuan and 17 other counties appeared extreme droughts and starvation, resulting in high amounts of hungry people. In 1909, severe spring and summer droughts in Gansu Province resulted in total crop failure, and countless people starved. Disaster victims were abundant in Weiyuan, Tongwei and Zhangxian. The situation was extremely dire. In 1928, an unprecedented spring and summer drought occurred in 65 counties of Gansu Province, and approximately two million people died of starvation. Historical records describe the land as being so dry, and it looked as if it had been burnt and could not grow crops. This drought was the worst in years for Dingxi, Lintao, Weiyuan, Tongwei and other counties. In 1945, Gansu Province also experienced a severe drought, particularly at Lintao, Weiyuan, Dingxi and Zhangxian. There were no summer crop yields and many people starved to death. The great drought event known as the "Ding-Wu famine," which resulted in about 30 million people deaths during the reign of Guangxu, and a serious drought during the late 1920s in northern China (Zheng *et al.,* 2014), were all recorded in the dry intervals of the reconstructed series. For the year 1923 in our series, relative drought records were not found in the SWR region. However, a heavy snowfall event occurred in September 2, 1922 in this region, and the snow reached approximately 666 mm, crushing small trees and big crowns (Compilation Committee of Tongwei County Annals, 1990), probably resulting in the narrower ring in 1923.

4.2 | Spatial representativeness and comparisons with other records

To show the spatial representation, spatial correlation analysis between the SWR precipitation and CRU TS4.00 grid

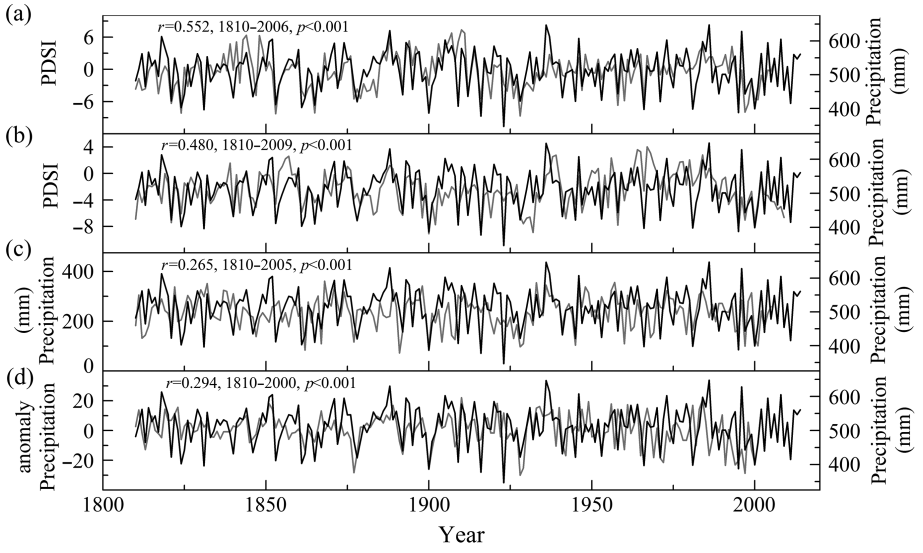

FIGURE 8 Comparisons between the reconstructed precipitation in the source region of Weihe River (SWR) and (a) PDSI at Mt. Guiqing (Fang *et al.,* 2010), (b) PDSI at Mt. Kongtong (Fang *et al.,* 2012), (c) precipitation at Mt. Huashan (Chen *et al.,* 2016; Sun and Liu, 2016) and (d) precipitation at West Qinling (Yang *et al.,* 2016)

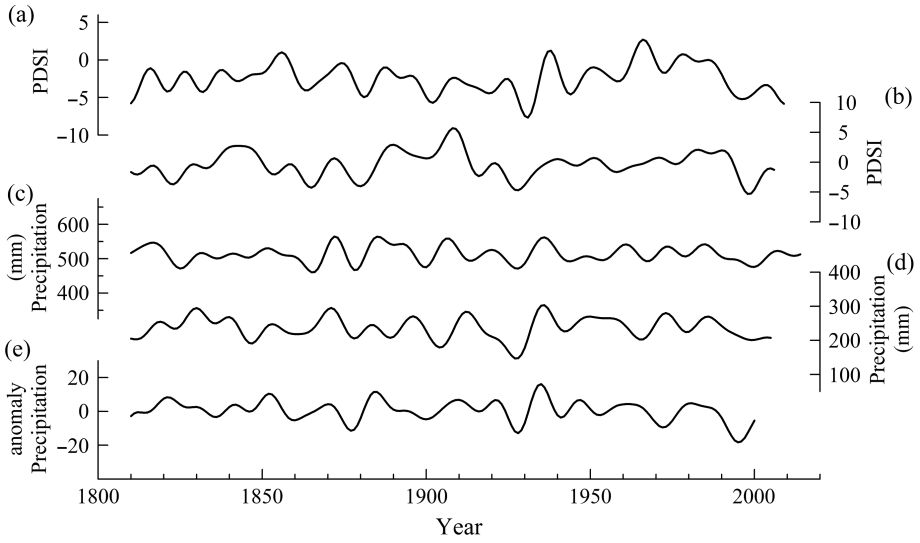

FIGURE 9 Comparisons of (a) the PDSI at Mt. Kongtong (Fang *et al.,* 2012), (b) PDSI at Mt. Guiqing (Fang *et al.,* 2010), (c) precipitation at this study site, (d) precipitation at Mt. Huashan (Chen *et al.,* 2016; Sun and Liu, 2016) and (e) precipitation at West Qinling (Yang *et al.,* 2016) after 10-year low-pass filter

precipitation was calculated during the period of 1958–2014 (Figure 7). The observed and reconstructed precipitation spatial patterns corresponded well, so the reconstructed series is a reliable proxy for large-scale precipitation.

To further test the spatial representation, we compared our reconstruction with two precipitation reconstruction series (Mt. Huashan and West Qinling) and two Palmer Drought Severity Index (PDSI) reconstructions (Mt. Guiqing and Mt. Kongtong) in adjacent areas of the SWR (Fang *et al.,* 2010; 2012; Chen *et al.,* 2016; Sun and Liu, 2016; Yang *et al.,* 2016). It might because the reconstructions belong to similar climate regions. The SWR precipitation not only had significant correlations with them at a high-frequency level (Figure 8), it also compared well with them after 10-year low-pass filter (Figure 9). Famous droughts in the late 1870s, the late 1920s and the late 20th century could all be found in these series, and these drought events all had some extent of spatial characteristics in northern China (Academy of Chinese Meteorological Science, 1981; Zhang *et al.,* 2003). These results also supported the reliability of our reconstruction. Nonconformities in the series existed during some periods, and they were probably caused by differences in microhabitats at the sampling site and/or the reconstruction of different seasons. In addition, the PDSI variations were not only related to precipitation but also affected by temperature (Sun and Ma, 2015).

4.3 | Possible driving mechanism for precipitation

The 2–8-year cycles in this series were similar to the periodicities of ENSO (Diaz and Markgraf, 2000), indicating that precipitation in the SWR was likely affected by ENSO. On basis of reconstructed ENSO events by Gergis and Fowler (2009) and observed events classified using the same percentile analysis method for the Oceanic Niño Index (http://www.cpc.ncep.noaa.gov/ products/analysis_monitoring/ensostuff/ensoyears.shtml), it was found that dry/wet years corresponded well with the El Niño/La Niña events (Table 2). For example, the extreme El Niño in 1997 led to "southern flood and northern drought" in China (Lau and Weng, 2001). When El Niño occurs, the sea-surface temperature in the equatorial east Pacific is higher, resulting in weakening of the Walker circulation and Hadley circulation in the west Pacific. Due to the weakening of the Hadley circulation, the intensity and location of the western pacific subtropical high are stronger and more southerly, respectively, and the convergence flow on its northern side becomes notably strong. Therefore, during some periods, there is more rainfall in southern China and less in northern

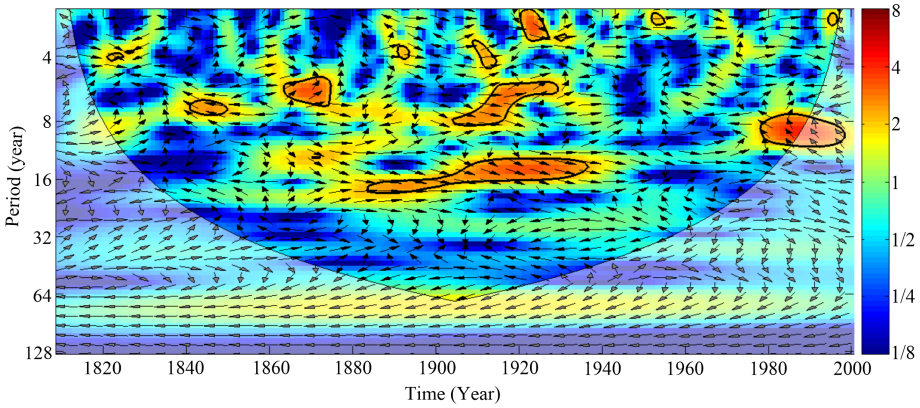

FIGURE 10 Wavelet coherence between the reconstructed precipitation and North Atlantic Oscillation (NAO) index (Luterbacher *et al.,* 2001). The black contour represents the 95% significance level, using a red-noise background spectrum. Arrows represent the phase of the coherence, where right is in phase and left is antiphase [Colour figure can be viewed at wileyonlinelibrary.com]

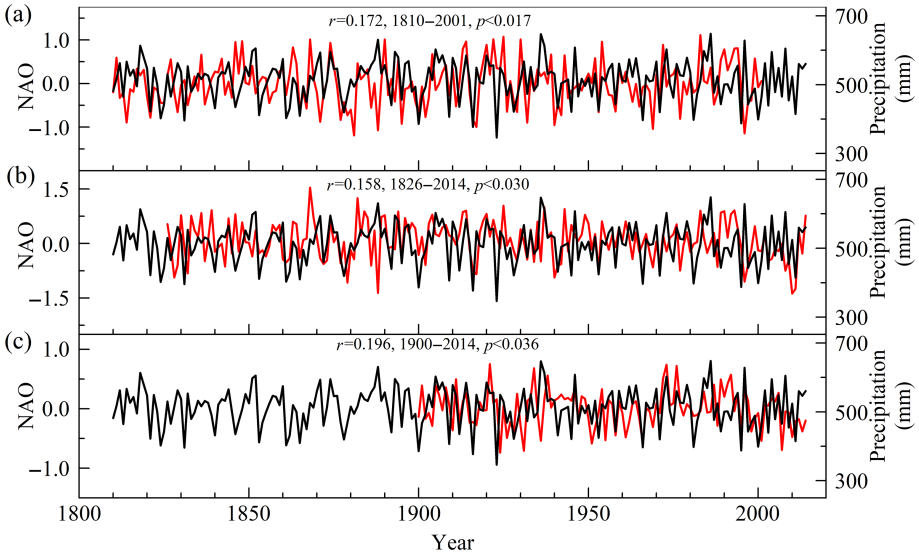

FIGURE 11 Comparisons between the reconstructed precipitation in the source region of Weihe River (SWR) and (a) the reconstructed NAO_{87} (Luterbacher *et al.,* 2001) based on the sea-level pressure from Trenbert and Paolino, (b) the observed NAO_{87} based on Iceland and Gibraltar pressure, and (c) the observed summer NAO_{87} based on the sea-level pressure from Trenbert and Paolino. NAO_{87} is the monthly mean North Atlantic Oscillation (NAO) index from previous August to current July [Colour figure can be viewed at wileyonlinelibrary.com]

TABLE 3 Correlations between the reconstructed P_{87} and monthly NAO from previous August to current July (NAO_{87})

NAO_{87}[a]		NAO_{87}[b]		NAO_{87}[c]	
Period	***r*, *p***	**Period**	***r*, *p***	**Period**	***r*, *p***
1900–2001	$r = 0.242$, $p < 0.014$	1900–2014	$r = 0.181$, $p < 0.053$	1900–2014	$r = 0.196$, $p < 0.036$
1850–2001	$r = 0.218$, $p < 0.007$	1850–2014	$r = 0.196$, $p < 0.014$		
1810–2001	$r = 0.172$, $p < 0.017$	1826–2014	$r = 0.158$, $p < 0.030$		

[a] Reconstructed NAO (Luterbacher *et al.,* 2001) based on the sea-level pressure from Trenbert and Paolino.

[b] Observed NAO based on Iceland and Gibraltar pressure.

[c] Observed summer NAO based on the sea-level pressure from Trenbert and Paolino.

China (Zou and Ni, 1997; Su and Wang, 2007). During La Niña phases, the situation reverses.

The 15.9-year and 18.6-year quasiperiods of reconstructed precipitation were approximate to the interdecadal changes of NAO (Fu and Zeng, 2005). In addition, NAO also has interannual periodicities (Zhang *et al.,* 2011b). Wavelet coherence analysis (Figure 10) showed that the reconstructed precipitation had some similar cycles as the NAO cycles at interannual and interdecadal time scales. Therefore, NAO might have a certain influence on the SWR precipitation. Both Figure 11 and Table 3 show that the monthly observed NAO index (http://climexp.knmi.nl/data/inao.dat) based on Iceland and Gibraltar pressures, the reconstructed NAO (Luterbacher *et al.,* 2001) based on the sea-level pressure from Trenbert and Paolino and the observed summer NAO (http://climexp.knmi.nl/data/isnao_ucar.dat), all have significant correlations with the SWR precipitation. In addition, NAO also compared well with our reconstructed precipitation after 10-year low-pass filter (Figure 12). During the late 1870s, the late 1920s and the late 20th century, NAO was in low period and our study region had less rainfall. Usually, NAO variation can cause the change of the North Atlantic circulation system which likely affects the west wind belt trough system. Therefore,

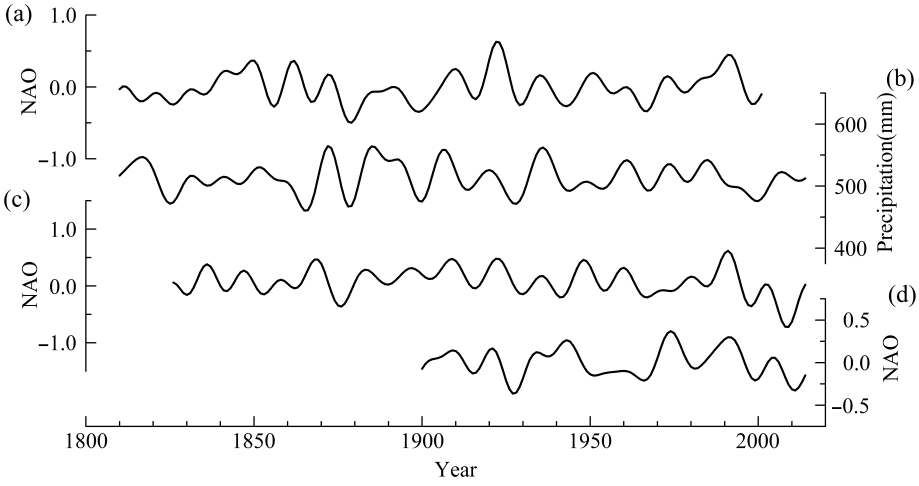

FIGURE 12 Comparisons of (a) the reconstructed North Atlantic Oscillation (NAO; Luterbacher *et al.,* 2001) based on the sea-level pressure from Trenbert and Paolino, (b) the reconstructed precipitation in this study, (c) the observed North Atlantic Oscillation (NAO) based on Iceland and Gibraltar pressure, and (d) the observed summer NAO based on the sea-level pressure from Trenbert and Paolino after 10-year low-pass filter

the climate in China is affected by NAO variations due to its downstream location ((Fu and Zeng, 2005). By influencing the tropospheric temperature changes, NAO can also affect the decadal variation of the Asian monsoon (Yu and Zhou, 2007), which plays an important role in climate change at northwest China.

5 | CONCLUSIONS

Using the tree-ring width chronology of *Picea purpurea* from Mt. Shouyang, the precipitation from previous August to current July since 1810 AD was reconstructed for the SWR, northwest China. The transfer function was stable and reliable, and the reconstruction could explain 42.6% of the variance of the observed precipitation over the calibration period of 1958–2014. During the past 205 years, there have been 33 dry years and 28 wet years. Many dry years corresponded to the dryness index in Lanzhou and could be supported by historical documents near the SWR. The famous drought event, the "Ding-Wu famine" during the reign of Guangxu and the serious drought in the late 1920s were well recorded in the dry intervals of the reconstruction. Spatial correlation patterns indicated that the reconstructed series could be representative of large-scale precipitation. Our reconstruction not only had significant correlations with other hydroclimate records in northwest China at high frequency, it also compared well with them at interdecadal scale. The 2–8-year cycles that are similar to the periodicities of ENSO and the 16–19-year quasiperiods that are similar to the interdecadal changes of NAO showed that ENSO and NAO had certain influences on the SWR precipitation change. When the El Niño/La Niña events occurred, dry/wet periods usually appeared in this region. During the low periods of NAO, the SWR often experienced droughts.

ACKNOWLEDGEMENTS

This study was supported by grants from the NSFC (41401060, 41630531), CAS Key Research Program of Frontier Sciences QYZDJ–SSW–DQC021 and XDPB05, GJHZ1777, Youth Innovation Promotion Association CAS, the Key Project of IEECAS and the Project of State Key Laboratory of Loess and Quaternary Geology (SKLLQG).

REFERENCES

Academy of Chinese Meteorological Science. (1981) *Yearly Charts of Dryness/-Wetness in China for the Last 500-year Period*. Beijing: China Map Press [in Chinese, with English abstract].

Chen, F., Yuan, Y.J., Wei, W.S., Zhang, R.B., Yu, S.L., Shang, H.M., Zhang, T.W., Qin, L., Wang, H.Q. and Chen, F.H. (2013) Tree-ring-based annual precipitation reconstruction for the Hexi Corridor, NW China: consequences for climate history on and beyond the mid-latitude Asian continent. *Boreas*, 42(4), 1008–1021. https://doi.org/10.1111/bor.12017.

Chen, F., Wang, H.Q., Chen, F.H., Yuan, Y.J. and Zhang, R.B. (2015) Tree-ring reconstruction of July-May precipitation (AD 1816–2010) in the northwestern marginal zone of the East Asian summer monsoon reveals the monsoon-related climate signals. *International Journal of Climatology*, 35(8), 2109–2121. https://doi.org/10.1002/joc.4110.

Chen, F., Zhang, R.B., Wang, H.Q., Qin, L. and Yuan, Y.J. (2016) Updated precipitation reconstruction (AD 1482–2012) for Huashan, north-central China. *Theoretical and Applied Climatology*, 123(3–4), 723–732. https://doi.org/10.1007/s00704-015-1387-0.

Compilation Committee of Dingxi County Annals. (1990) *Dingxi County Annals*. Lanzhou: Gansu People Publishing House [in Chinese].

Compilation Committee of Lintao County Annals. (2001) *Lintao County Annals*. Lanzhou: Gansu People Publishing House [in Chinese].

Compilation Committee of Longxi County Annals. (1990) *Longxi County Annals*. Lanzhou: Gansu People Publishing House [in Chinese].

Compilation Committee of Tongwei County Annals. (1990) *Tongwei County Annals*. Lanzhou: Lanzhou University Press [in Chinese].

Compilation Committee of Weiyuan County Annals. (1998) *Weiyuan County Annals*. Lanzhou: Lanzhou University Press [in Chinese].

Compilation Committee of Zhangxian County Annals. (2005) *Zhangxian County Annals*. Lanzhou: Gansu Culture Publishing House [in Chinese].

Cook, E.R. (1985) *A time-series analysis approach to tree-ring standardization*. Dissertation, The University of Arizona, Tucson, AZ.

Cook, E.R. and Kairiukstis, L.A. (1990) *Methods of Dendrochronology*. Dordrecht: Kluwer Academic.

Cook, E.R., Meko, D.M., Stahle, D.W. and Cleaveland, M.K. (1999) Drought reconstructions for the continental United States. *Journal of Climate*, 12(4), 1145–1162.

Diaz, H.F. and Markgraf, V. (2000) *El Niño and the Southern Oscillation: Multiscale Variability and Global and Regional Impacts*. Cambridge: Cambridge University Press.

Fang, K.Y., Gou, X.H., Chen, F.H., D'Arrigo, R. and Li, J.B. (2010) Tree-ring based drought reconstruction for the Guiqing Mountain (China): linkages to the Indian and Pacific oceans. *International Journal of Climatology*, 30(8), 1137–1145.

Fang, K.Y., Gou, X.H., Chen, F.H., Liu, C.Z., Davi, N., Li, J.B., Zhao, Z.Q. and Li, Y.J. (2012) Tree-ring based reconstruction of drought variability (1615–2009) in the Kongtong Mountain area, northern China. *Global and Planetary Change*, 80–81, 190–197. https://doi.org/10.1016/j.gloplacha.2011.10.009.

Fritts, H.C. (1976) *Tree Rings and Climate*. London: Elsevier. https://doi.org/10.1016/B978-0-12-268450-0.50016-1.

Fu, C.B. and Zeng, Z.M. (2005) Relationship between the winter North Atlantic Oscillation and the summer variations of dryness/wetness in eastern China during the last 530 years. *Chinese Science Bulletin*, 50(14), 1512–1522.

Gao, J.X., Shi, Z.J., Xu, L.H., Yang, X.H., Jia, Z.Q., Lu, S.H., Feng, C.Y. and Shang, J.X. (2013) Precipitation variability in Hulunbuir, northeastern China since 1829 AD reconstructed from tree-rings and its linkage with remote oceans. *Journal of Arid Environments*, 95, 14–21. https://doi.org/10.1016/j.jaridenv.2013.02.011.

Gergis, J.L. and Fowler, A.M. (2009) A history of ENSO events since AD 1525: implications for future climate change. *Climatic Change*, 92(3–4), 343–387. https://doi.org/10.1007/s10584-008-9476-z.

Gou, X.H., Gao, L.L., Deng, Y., Chen, F.H., Yang, M.X. and Still, C. (2015) An 850-year tree-ring-based reconstruction of drought history in the western Qilian Mountains of northwestern China. *International Journal of Climatology*, 35(11), 3308–3319. https://doi.org/10.1002/joc.4208.

Holmes, R.L. (1983) Computer-assisted quality control in tree-ring dating and measurement. *Tree-Ring Bulletin*, 44(3), 69–75.

Lau, K.M. and Weng, H.Y. (2001) Coherent modes of global SST and summer rainfall over China: an assessment of the regional impacts of the 1997-98 El Nino. *Journal of Climate*, 14(6), 1294–1308. https://doi.org/10.1175/1520-0442(2001)014<1294:Cmogsa>2.0.Co;2.

Li, J.B., Gou, X.H., Cook, E.R. and Chen, F.H. (2006a) Tree-ring based drought reconstruction for the central Tien Shan area in northwest China. *Geophysical Research Letters*, 33(7), L07715. https://doi.org/10.1029/2006gl025803.

Li, Q., Liu, Y., Cai, Q.F., Sun, J.Y., Yi, L., Song, H.M. and Wang, L. (2006b) Reconstruction of annual precipitation since 1686 AD from Ningwu region, Shanxi Province. *Journal of Quaternary Science*, 26(6), 999–1006 [in Chinese, with English abstract].

Li, Q., Liu, Y., Song, H., Yang, Y. and Zhao, B. (2015) Divergence of tree-ring-based drought reconstruction between the individual sampling site and the monsoon Asia drought atlas: an example from Guancen Mountain. *Scientific Bulletin*, 60(19), 1688–1697.

Liu, Y., Cai, Q.F., Shi, J.F., Hughes, M.K., Kutzbach, J.E., Liu, Z.Y., Ni, F.B. and An, Z.S. (2005) Seasonal precipitation in the south-central Helan Mountain region, China, reconstructed from tree-ring width for the past 224 years. *Canadian Journal of Forest Research*, 35(10), 2403–2412.

Liu, Y., Tian, H., Song, H.M. and Liang, J.M. (2010) Tree ring precipitation reconstruction in the Chifeng-Weichang region, China, and East Asian summer monsoon variation since AD 1777. *Journal of Geophysical Research – Atmospheres*, 115, D06103. https://doi.org/10.1029/2009JD012330.

Liu, Y., Wang, C.Y., Hao, W.J., Song, H.M., Cai, Q.F., Tian, H., Sun, B. and Linderholm, H.W. (2011) Tree-ring-based annual precipitation reconstruction in Kalaqin, Inner Mongolia for the last 238 years. *Chinese Science Bulletin*, 56(28–29), 2995–3002.

Liu, Y., Lei, Y., Sun, B., Song, H.M. and Sun, J.Y. (2013a) Annual precipitation in Liancheng, China, since 1777 AD derived from tree rings of Chinese pine (Pinus tabulaeformis Carr.). *International Journal of Biometeorology*, 57(6), 927–934.

Liu, Y., Sun, B., Song, H.M., Lei, Y. and Wang, C.Y. (2013b) Tree-ring-based precipitation reconstruction for Mt. Xinglong, China, since AD 1679. *Quaternary International*, 283, 46–54.

Luterbacher, J., Xoplaki, E., Dietrich, D., Jones, P.D., Davies, T.D., Portis, D., Gonzalez-Rouco, J.F., von Storch, H., Gyalistras, D., Casty, C. and Wanner, H. (2001) Extending North Atlantic Oscillation reconstructions back to 1500. *Atmospheric Science Letters*, 2(1–4), 114–124. https://doi.org/10.1006/asle.2001.0044.

Meko, D. and Graybill, D.A. (1995) Tree-ring reconstruction of Upper Gila River discharge. *Water Resources Bulletin*, 31(4), 605–616.

Peng, J.J., Sun, Y., Chen, M., He, X.Y., Davi, N.K., Zhang, X.L., Li, T., Zhu, C.Y., Cai, C. and Chen, Z.J. (2013) Tree-ring based precipitation variability since AD 1828 in northwestern Liaoning, China. *Quaternary International*, 283, 63–71.

Scaife, A.A., Knight, J.R., Vallis, G.K. and Folland, C.K. (2005) A stratospheric influence on the winter NAO and North Atlantic surface climate. *Geophysical Research Letters*, 32(18), L18715. https://doi.org/10.1029/2005gl023226.

Song, C.S. and Wang, C.R. (2002) *Scientific Survey of Gansu Lianhuashan Natural Reserve*. Beijing: China Forestry Publishing House [in Chinese].

Song, H.M., Liu, Y., Li, Q. and Linderholm, H. (2013) Tree-ring derived temperature records in the central Loess Plateau, China. *Quaternary International*, 283, 30–35.

Su, M.F. and Wang, H.J. (2007) Relationship and its instability of ENSO - Chinese variations in droughts and wet spells. *Science in China. Series D*, 50(1), 145–152. https://doi.org/10.1007/s11430-007-2006-4.

Sun, J.Y. and Liu, Y. (2012) Tree ring based precipitation reconstruction in the south slope of the middle Qilian Mountains, northeastern Tibetan Plateau, over the last millennium. *Journal of Geophysical Research – Atmospheres*, 117, D08108. https://doi.org/10.1029/2011jd017290.

Sun, C.F. and Liu, Y. (2016) Climate response of tree radial growth at different timescales in the Qinling Mountains. *PLoS One*, 11(8), e0160938. https://doi.org/10.1371/journal.pone.0160938.

Sun, C.F. and Ma, Y.Y. (2015) Effects of non-linear temperature and precipitation trends on Loess Plateau droughts. *Quaternary International*, 372, 175–179.

Thomson, D.J. (1982) Spectrum estimation and harmonic-analysis. *Proceedings of the IEEE*, 70(9), 1055–1096. https://doi.org/10.1109/Proc.1982.12433.

Tian, Q.H., Zhou, X.J., Gou, X.H., Zhao, P., Fan, Z.X. and Helama, S. (2012) Analysis of reconstructed annual precipitation from tree-rings for the past 500 years in the middle Qilian Mountain. *Science China Earth Sciences*, 55(5), 770–778. https://doi.org/10.1007/s11430-012-4375-6.

Torrence, C. and Compo, G.P. (1998) A practical guide to wavelet analysis. *Bulletin of the American Meteorological Society*, 79, 61–78.

Wang, B. (2006) *The Asian Monsoon*. Berlin and Heidelberg: Springer. https://doi.org/10.1007/3-540-37722-0.

Wang, H. (2009) *Response of runoff and sediment to land-use change in Wei River source region.* Dissertation, Lanzhou University, Lanzhou [in Chinese, with English abstract].

Wang, H.J., Chen, Y.N., Pan, Y.P. and Li, W.H. (2015) Spatial and temporal variability of drought in the arid region of China and its relationships to teleconnection indices. *Journal of Hydrology*, 523, 283–296. https://doi.org/10.1016/j.jhydrol.2015.01.055.

Wigley, T.M.L., Briffa, K.R. and Jones, P.D. (1984) On the average value of correlated time series, with application in dendroclimatology and hydrometeorology. *Journal of Climate and Applied Meteorology*, 23, 201–213.

Wu, Z.H., Huang, N.E. and Chen, X.Y. (2009) The multi-dimensional ensemble empirical mode decomposition method. *Advances in Adaptive Data Analysis*, 1(3), 339–372.

Yang, B., Qin, C., Brauning, A., Burchardt, I. and Liu, J.J. (2011) Rainfall history for the Hexi Corridor in the arid northwest China during the past 620 years derived from tree rings. *International Journal of Climatology*, 31(8), 1166–1176. https://doi.org/10.1002/joc.2143.

Yang, F., Wang, N., Shi, F., Ljungqvist, F.C., Zhao, S. and Liu, T. (2016) The spatial distribution of precipitation over the West Qinling region, China, AD 1470–2000. *Palaeogeography, Palaeoclimatology, Palaeoecology*, 443, 278–285. https://doi.org/10.1016/j.palaeo.2015.12.003.

Yao, Y.B., Zhang, X.Y., Duan, Z.Y., Song, Y.J., Yang, J.J. and Wang, D.J. (2011) Climate Evolution and Its Impact to Water Resource Changer in Source of Weihe River Basin. *Agricultural Research In The Arid Areas*, 29(5), 247–252 [in Chinese, with English abstract].

Yu, R.C. and Zhou, T.J. (2007) Seasonality and three-dimensional structure of interdecadal change in the East Asian monsoon. *Journal of Climate*, 20(21), 5344–5355. https://doi.org/10.1175/2007JCLI1559.1.

Zhang, D.E., Li, X.Q. and Liang, Y.Y. (2003) Supplement for "Yearly charts of dryness/wetness in China for the last 500-year period". *Journal of Applied Meteorological Science*, 14(3), 379–388 [in Chinese, with English abstract].

Zhang, Y., Tian, Q.H., Gou, X.H., Chen, F.H., Leavitt, S.W. and Wang, Y.S. (2011a) Annual precipitation reconstruction since AD 775 based on tree rings from the Qilian Mountains, northwestern China. *International Journal of Climatology*, 31(3), 371–381. https://doi.org/10.1002/joc.2085.

Zhang, X.J., Jin, L.Y., Chen, C.Z., Guan, D.S. and Li, M.Z. (2011b) Interannual and interdecadal variations in the North Atlantic Oscillation spatial shift. *Chinese Science Bulletin*, 56(24), 2621–2627. https://doi.org/10.1007/s11434-011-4607-8.

Zhang, T.W., Yuan, Y.J., Liu, Y., Wei, W.S., Zhang, R.B., Chen, F., Yu, S.L., Shang, H.M. and Qin, L. (2013) A tree-ring based temperature reconstruction for the Kaiduhe River watershed, northwestern China, since AD 1680: linkages to the North Atlantic Oscillation. *Quaternary International*, 311, 71–80.

Zhang, T.W., Yuan, Y.J., Wei, W.S., Yu, S.L., Zhang, R.B., Chen, F., Shang, H.M. and Qin, L. (2014) A tree-ring based precipitation reconstruction for the Mohe region in the northern Greater Higgnan Mountains, China, since AD 1724. *Quaternary Research*, 82(1), 14–21.

Zheng, J.Y., Hao, Z.X., Fang, X.Q. and Ge, Q.S. (2014) Changing characteristics of extreme climate events during past 2000 years in China. *Progress in Geography*, 33(1), 3–12 [in Chinese, with English abstract].

Zou, L. and Ni, Y.Q. (1997) Impact of ENSO on the variability of the summer monsoon over Asia and the summer rainfall. *Journal of Tropical Meteorology*, 13(4), 306–314 [in Chinese, with English abstract].

How to cite this article: Sun C, Liu Y, Song H, *et al.* Tree-ring-based precipitation reconstruction in the source region of Weihe River, northwest China since AD 1810. *Int J Climatol*. 2018;38:3421–3431. https://doi.org/10.1002/joc.5514